Metallaheteroborane Chemistry. Part 9.[1] Syntheses and Spectroscopy of Platinum and Palladium Phosphine Complexes containing η^5-$\{As_2B_9\}$-based Cluster Ligands. Crystal Structures of [3,3-L_2-*closo*-3,1,2-$PtAs_2B_9H_9$] (L = PPh_3 or PMe_2Ph) and [3-Cl-3,8-$(PPh_3)_2$-*closo*-3,1,2-$PdAs_2B_9H_8$]†

Marguerite McGrath,[a] Trevor R. Spalding,*[a] Xavier L. R. Fontaine,[b] John D. Kennedy[b] and Mark Thornton-Pett[b]

[a] *Chemistry Department, University College, Cork, Ireland*

[b] *School of Chemistry, University of Leeds, Leeds LS2 9JT, UK*

The reaction between $[Pt(PPh_3)_4]$ and *closo*-1,2-$As_2B_{10}H_{10}$ in ethanol gives [3,3-$(PPh_3)_2$-*closo*-3,1,2-$PtAs_2B_9H_9$] **1** in low yield (9%). Reaction of [*nido*-7,8-$As_2B_9H_{10}$]$^-$ and $[MCl_2(PR_3)_2]$ in tetrahydrofuran(thf) in the presence of a ten-fold excess of NEt_3 affords [3,3-$(PR_3)_2$-*closo*-3,1,2-$MAs_2B_9H_9$] (M = Pt, R_3 = Me_2Ph **2**; M = Pd, R_3 = Ph_3 **3** or Me_2Ph **4**) and [3-Cl-3,8-$(PR_3)_2$-*closo*-3,1,2-$PdAs_2B_9H_8$] (R_3 = Ph_3 **5**; or R_3 = Me_2Ph, **6**) in low-to-moderate (20–45%) yields. X-Ray diffraction analyses of **1**, **2** and **5** confirm the *closo* icosahedral MAs_2B_9 cage structures and the presence of a MAs_2 triangulated face in each of these molecules. Both compounds **1** and **2** crystallise in the monoclinic space group $P2_1/n$ with $Z = 4$. Cell dimensions: **1**, a = 1230.0(2), b = 1736.5(4), c = 1881.0(3) pm and β = 91.44(2)°; **2**, a = 1308.6(3), b = 1058.0(2), c = 1934.7(3) pm and β = 104.45(2)°. The structure of **1** was refined to a final R of 0.0574 (R' 0.0532) for the 4160 reflections with $I \geqslant 2.0\sigma(I)$. One of the As atoms is disordered over two sites. Calculated Pt–As distances are 259.1(5), 255.7(5) and 264.0(6) pm, As–As 251.5(6) and 243.5(5) pm. Structure **2** had a final R of 0.0384 (R' 0.0376) for the 3778 reflections with $I \geqslant 2.0\sigma(I)$. The Pt–As distances are 265.5(4) and 254.5(4) pm and As–As is 249.7(3) pm. Compound **5** crystallises in the triclinic space group $P\bar{1}$ with $Z = 2$, a = 1037.8(2), b = 1321.9(3), c = 1712.9(3) pm, α = 103.67(1), β = 93.19(1) and γ = 110.86(1)°; final R = 0.0392 (R' = 0.0408) for 4688 reflections with $I \geqslant 2.0\sigma(I)$. The Pd–As distances are 256.3(4) and 253.9(4) pm and As–As is 247.7(3) pm. Compounds **1**–**6** were characterised by multielement NMR spectroscopy. Variable-temperature ^1H studies of **2**, **4** and **6** show the metal to As_2B_9 ligand bonding is fluxional at room temperature with $\Delta G^{\ddagger}_{298} < ca.$ 30 kJ mol^{-1} for **2** and **4** and possibly slightly higher for **6** at *ca.* 32 kJ mol^{-1}. An analysis of the frontier molecular orbitals of the model ligand $P_2B_9H_9$ and their possible interactions with a $Pt(PH_3)_2$ group shows no clear preference between the two possible conformations that the PtP_2 unit could adopt above the P_2B_3 face to which it bonds.

The eleven-vertex diarsenaborane anion [*nido*-7,8-$As_2B_9H_{10}$]$^-$ was prepared first by Little *et al.*[2] in 1974. Subsequently a number of first-row transition-metal complexes containing the $As_2B_9H_9$ ligand were prepared including [3-(η^5-C_5H_5)-3,1,2-$CoAs_2B_9H_9$][3] and [3-($Ph_2PCH_2CH_2PPh_2$)-3,1,2-$NiAs_2B_9H_9$].[4] In a continuation of our studies of metallaheteroboranes,[5–7] which recently included some rhodadiarsenaboranes,[1] we decided to synthesise some platinum and palladium phosphine complexes with As_2B_9-cluster ligands. This paper reports the syntheses of the twelve-vertex complexes [3,3-$(PR_3)_2$-*closo*-3,1,2-$MAs_2B_9H_9$] (M = Pt, R_3 = Ph_3 **1** or Me_2Ph **2**; M = Pd, R_3 = Ph_3 **3** or Me_2Ph **4**) and [3-Cl-3,8-$(PR_3)_2$-*closo*-3,1,2-$PdAs_2B_9H_8$] (R_3 = Ph_3 **5** or Me_2Ph **6**). These complexes were investigated with multielemental NMR spectroscopy and, in the cases of representative compounds **1**, **2** and **5**, single-crystal X-ray diffraction analyses were performed. The results are discussed with reference to related known *closo* twelve-vertex cluster compounds of the types [2,2-$(PR_3)_2$-2,1-$PtXB_{10}H_{10}$] (R_3 = Et_3, Bu^n_3 or Me_2Ph; X = Se or Te)[5,7] and [3,3-L_2-3,1,2-$MC_2B_9H_{11}$] [M = Pt, L = PEt_3;[8] M = Pd, L = $\frac{1}{2}Me_2NCH_2CH_2NMe_2$ (tmen), PMe_3, $P(OMe)_3$, $\frac{1}{2}Ph_2PCH_2CH_2PPh_2$ (dppe), Bu^tNC,[9] or cycloocta-1,5-diene (cod)[9,10]].

† 3,3-Bis(triphenylphosphine)- and 3,3-bis(dimethylphenylphosphine)-1,2-diarsa-3-platina-*closo*-dodecaborane and 3-chloro-3,8-bis(triphenylphosphine)-1,2-diarsa-3-platina-*closo*-dedecaborane.

Supplementary data available: see Instructions for Authors, *J. Chem. Soc., Dalton Trans.*, 1991, Issue 1, pp. xviii–xxii.

Non-SI unit employed: eV ≈ 1.60 × 10^{-19} J.

Results and Discussion

(1) *Preparation of Compounds* **1**–**6**.—The reaction between $[Pt(PPh_3)_4]$ and *closo*-1,2-$As_2B_{10}H_{10}$ in refluxing absolute ethanol solution for 24 h proceeded with formal excision of a BH group and formal oxidation of platinum to afford [3,3-$(PPh_3)_2$-*closo*-3,1,2-$PtAs_2B_9H_9$] **1** in low yield (9.3%). All other complexes in the present study were synthesised by salt-elimination reactions using the general procedure of allowing complexes of general formula $[MCl_2(PR_3)_2]$ to react with $[NMe_4]$[*nido*-7,8-$As_2B_9H_{10}$] in a 1:1 mole ratio in tetrahydrofuran (thf) solution in the presence of a ten-fold excess of triethylamine, equation (1).

$$[MCl_2(PR_3)_2] + [As_2B_9H_{10}]^- + NEt_3 \longrightarrow [NHEt_3]Cl + Cl^- + [(PR_3)_2MAs_2B_9H_9] \quad (1)$$

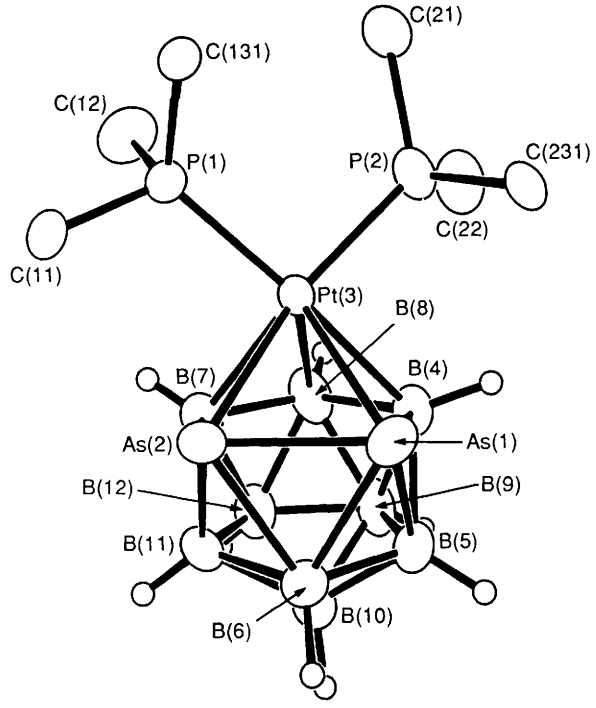

Fig. 1 An ORTEP-type diagram of [3,3-$(PMe_2Ph)_2$-*closo*-3,1,2-$PtAs_2B_9H_9$] **2** with P-organyl atoms, other than those attached to phosphorus, omitted for clarity

The reaction mixture with the *cis* platinum reagent (R_3 = Me_2Ph) was initially stirred at room temperature for 2 d and subsequently heated at reflux for 6 h. Chromatographic separation of the products and crystallisation of the only major product afforded red crystals of [3,3-$(PMe_2Ph)_2$-*closo*-3,1,2-$PtAs_2B_9H_9$], **2** (44.6%). The reaction with $[PdCl_2(PPh_3)_2]$ was initially carried out at room temperature for 2 d. Two products were isolated by chromatography, lavender crystals of [3,3-$(PPh_3)_2$-*closo*-3,1,2-$PdAs_2B_9H_9$] **3** (31.4%) and emerald-green crystals of [3-Cl-3,8-$(PPh_3)_2$-*closo*-3,1,2-$PdAs_2B_9H_8$] **5** (1.1%). When this reaction was carried out at room temperature for 16 h, followed by heating at reflux for 20 min, the same products, **3** and **5**, were isolated but in 1.5 and 26.8% yield respectively. The reaction with $[PdCl_2(PMe_2Ph)_2]$ for 36 h at room temperature afforded lavender [3,3-$(PMe_2Ph)_2$-*closo*-3,1,2-$PdAs_2B_9H_9$] **4** (40.5%) and green [3-Cl-3,8-$(PMe_2Ph)_2$-*closo*-3,1,2-$PdAs_2B_9H_8$] **6** (19.7%).

From these results it would appear that, as far as the metal-centred moiety is concerned, the general effect of capping the As_2B_9 cage is the removal of two adjacent (*cis*) ligands from either the *cis*- or *trans*-$[MCl_2(PR_3)_2]$ complexes. In the case of the *cis* platinum complex the product is formed only when two chloride ligands are removed. In the palladium cases, where the reagents are known to be mixtures of *cis* and *trans* complexes,[11] removal of either (*a*) two chloride or (*b*) one chloride and one phosphine ligand is possible. Clearly the factors affecting the differences in the reactivities of the metal reagents are complex. A number of features may be important including (*a*) the *cis*/*trans* ratio in the reagent complexes (especially the palladium compounds), (*b*) the effect of NEt_3 as an isomerisation catalyst, and (*c*) the expected greater rate of the substitution and isomerisation reactions of palladium complexes compared to the equivalent platinum compounds. Kinetic and mechanistic studies of these reactions would be required to assess the relative importance of these effects.

All compounds **1**–**6** were initially characterised by their infrared spectra in KBr discs. All contained absorptions in the phosphine and borane regions. The borane bands were as follows: **1** 2520s; **2** 2530vs, 2505vs(sh), 2495vs(sh); **3** 2525vs; **4** 2558s(sh), 2520vs, 2488s(sh); **5** 2560s, 2539s, 2510s(sh); **6** 2550s, 2540s and 2517vs cm^{-1}.

Table 1 Selected interatomic distances (pm) and angles (°) for compound **2**

As(1)–Pt(3)	265.5(4)	As(2)–Pt(3)	254.5(4)
P(1)–Pt(3)	230.0(4)	P(2)–Pt(3)	229.4(4)
B(4)–Pt(3)	227.9(11)	B(7)–Pt(3)	228.9(11)
B(8)–Pt(3)	228.1(12)		
As(2)–As(1)	249.7(3)	B(4)–As(1)	220.9(11)
B(5)–As(1)	211.6(13)	B(6)–As(1)	223.1(11)
B(6)–As(2)	225.7(11)	B(7)–As(2)	225.3(12)
B(11)–As(2)	210.4(12)		
B(5)–B(4)	186.1(16)	B(8)–B(4)	183.3(16)
B(9)–B(4)	175.1(15)	B(9)–B(5)	177.2(18)
B(6)–B(5)	177.4(17)	B(11)–B(6)	183.9(17)
B(10)–B(5)	176.3(17)	B(8)–B(7)	180.4(15)
B(10)–B(6)	173.0(17)	B(12)–B(7)	175.1(16)
B(11)–B(7)	184.6(15)	B(9)–B(8)	175.8(17)
B(12)–B(8)	177.7(15)	B(12)–B(9)	176.0(16)
B(10)–B(9)	176.2(16)	B(11)–B(10)	177.9(16)
B(12)–B(10)	176.1(19)	B(12)–B(11)	174.6(17)
C(11)–P(1)	181.8(11)	C(21)–P(2)	181.7(11)
C(12)–P(1)	181.4(11)	C(22)–P(2)	180.9(11)
C(131)–P(1)	181.4(7)	C(231)–P(2)	181.7(7)

Angles at Pt(3), As(1), As(2), P(1) and P(2)

As(1)–Pt(3)–As(2)	57.4(3)	C(11)–P(1)–Pt(3)	116.8(4)
As(2)–Pt(3)–B(7)	55.2(3)	C(12)–P(1)–Pt(3)	110.2(5)
B(7)–Pt(3)–B(8)	46.5(3)	C(131)–P(1)–Pt(3)	119.3(3)
B(8)–Pt(3)–B(4)	47.4(3)	C(21)–P(2)–Pt(3)	121.1(4)
As(1)–Pt(3)–B(4)	52.5(3)	C(22)–P(2)–Pt(3)	113.4(4)
P(1)–Pt(3)–P(2)	96.5(2)	C(231)–P(2)–Pt(3)	112.1(3)
As(2)–As(1)–Pt(3)	59.1(4)	As(1)–As(2)–Pt(3)	63.5(4)
B(4)–As(1)–Pt(3)	55.0(3)	As(1)–As(2)–B(6)	55.7(4)
B(4)–As(1)–B(5)	50.9(5)	B(6)–As(2)–B(11)	49.7(4)
B(5)–As(1)–B(6)	48.1(4)	B(7)–As(2)–B(11)	50.0(5)
As(2)–As(1)–B(6)	56.7(3)	B(7)–As(2)–Pt(3)	56.6(3)

Angles in the As(1)As(2)B(7)B(8)B(4), Pt(3)B(4)B(5)B(6)As(2) and Pt(3)As(1)B(6)B(11)B(7) rings below Pt(3), As(1) and As(2) respectively

As(1)–As(2)–B(7)	98.4(4)	B(8)–B(4)–As(1)	121.4(7)
As(2)–B(7)–B(8)	116.6(7)	B(4)–As(1)–As(2)	93.8(3)
B(7)–B(8)–B(4)	109.7(8)		
As(2)–Pt(3)–B(4)	90.9(3)	Pt(3)–As(1)–B(6)	98.6(4)
Pt(3)–B(4)–B(5)	120.4(7)	As(1)–B(6)–B(11)	114.6(6)
B(4)–B(5)–B(6)	112.3(8)	B(6)–B(11)–B(7)	115.5(7)
B(5)–B(6)–As(2)	114.5(7)	B(11)–B(7)–Pt(3)	116.9(7)
B(6)–As(2)–Pt(3)	101.2(4)	B(7)–Pt(3)–As(1)	93.1(3)

Since no solid-state structures of platina- or palladaarsenaboranes had been reported, it was decided to undertake single-crystal X-ray diffraction analyses of compounds **1**, **2** and **5**. Suitable crystals were grown from dichloromethane solutions of **1** and **5**, and from a dichloromethane–*cyclo*hexane (3:1) solution of **2**. The results of these analyses are discussed in the order **2**, **1** and **5**.

(2) *Molecular Structure of* [3,3-$(PMe_2Ph)_2$-closo-3,1,2-$PtAs_2B_9H_9$] **2**.—The molecular structure of [3,3-$(PMe_2Ph)_2$-*closo*-3,1,2-$PtAs_2B_9H_9$] **2** is shown in Fig. 1, and important interatomic distances and angles are given in Table 1. The *closo*-$PtAs_2B_9$ geometry is that of a distorted icosahedron with the platinum and two arsenic atoms forming one triangular face. In terms of Wade's analysis of clusters,[12] the molecule is a derivative of $[closo\text{-}B_{12}H_{12}]^{2-}$ with the $Pt(PMe_2Ph)_2$ unit and the two arsenic atoms notionally replacing BH and two $[BH]^-$ units respectively.

The platinum–arsenic distances are significantly different, Pt–As(1) and Pt–As(2) being 265.5(4) and 254.5(4) pm respectively. The reason is not clear, especially since all the platinum–boron distances are the same within experimental error [Pt–B(4) 227.9(11), Pt–B(7) 228.9(11) and Pt–B(8) 228.1(12) pm] as are the platinum–phosphorus distances

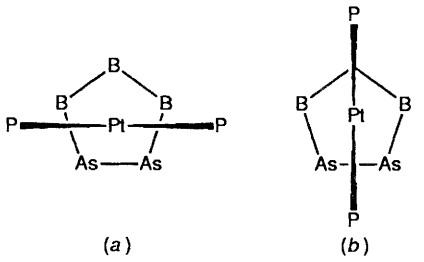

Fig. 2 Possible conformations of the PtP_2 unit above the As_2B_3 face of the $\{As_2B_9H_9\}$ ligand: (*a*) 'Planes parallel', (*b*) 'planes perpendicular'

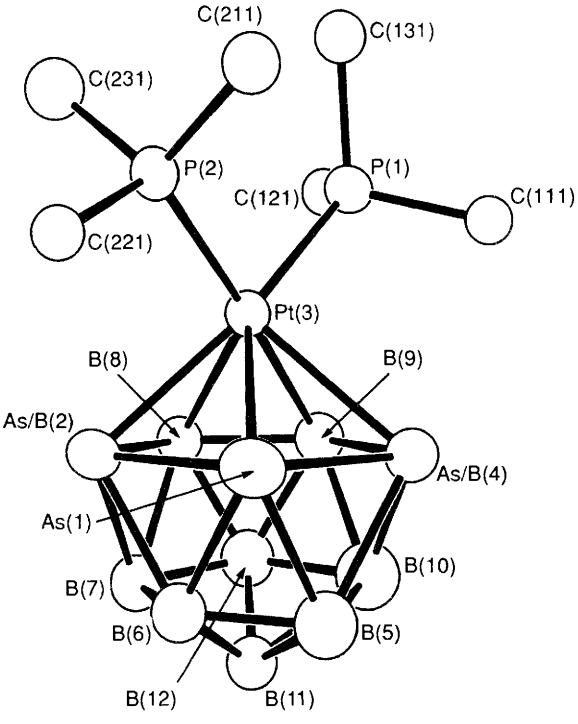

Fig. 3 An ORTEP-type diagram of $[3,3\text{-}(PPh_3)_2\text{-}closo\text{-}3,1,2\text{-}PtAs_2B_9H_9]$ **1** with P-organyl atoms, other than those attached to phosphorus, omitted for clarity

[Pt–P(1) 230.0(4) and Pt–P(2) 229.4(4) pm]; also there is no concomitant markedly large variation in the corresponding boron–arsenic distances. Of the three arsenic–boron distances for each arsenic atom, one is shorter than the other two. For As(1) the distance to B(5) [211.6(13)] pm is shorter than those to B(4) and B(6) [220.9(11) and 223.1(11) pm]. For As(2) the related distances are 210.4(12) to B(11), 225.3(12) to B(7) and 225.7(11) pm to B(6). Thus, comparable arsenic to boron distances involving boron atoms bonded to two heteroatoms (As or Pt) are significantly longer than those involving only one arsenic interaction. Similar observations have been made in twelve-atom *closo* MXB_{10} clusters, where MX = PtTe,[5] PtSe[7] or RhTe.[6]

The boron–boron distances in compound **2** are in the range 173.0(17) to 186.1(16) pm which is not unusually large for metalla-boranes and -heteroboranes.[13] The two longest inter-boron distances involve atoms B(4) and B(7) which are bonded to both platinum and arsenic atoms. The shortest distance is between B(6) and B(10), Table 1.

Comparison of the platinum–arsenic distances in **2** [265.5(4) and 254.5(4) pm] with those in non-cage molecules reveals them to be longer. Typical Pt–AsR_3 distances are from 227.5(2) pm in [1-(*o*-diphenylarsinophenyl)-2-methoxyethyl-*As*,*C*^{1}](hexafluoroacetylacetonato)platinum(II)[14] to 243.6(1) pm in tetrafluoroethylenebis(triphenylarsine) platinum(0).[15]

The interarsenic distance in compound **2** [249.7(3) pm] is close to the values for two-electron two-centre As···As distances for which the 'normal' range of 243–246 pm has been suggested.[16]

The conformation of the PtP_2 unit above the As_2B_3 face of the arsenaborane ligand in compound **2** is analogous to that found in the solid-state structures of 3,1,2-PtC_2B_9 carbaboranes, where the plane containing the PtP_2 atoms is perpendicular to the C_2B_3 face and parallel to a plane containing the two carbon atoms [Fig. 2(*a*) 'planes parallel']. The alternative conformation, 'planes perpendicular', is shown in Fig. 2(*b*). The platinum–carbaborane interaction has been analysed in terms of the frontier orbitals of the $\{Pt(PH_3)_2\}$ and $\{C_2B_9H_{11}\}$ species.[8] We have attempted a similar analysis for the present compounds using the model ligand $\{P_2B_9H_9\}$ and the minimum neglect of differential overlap (MNDO) molecular orbital calculation programme. The results of the calculations indicate that the interaction of PtP_2 with the P_2B_3 face of $P_2B_9H_9$ may not be the same as that with the C_2B_3 face of the carbaborane ligand. In the case of the platinacarbaborane, the conformation-determining molecular orbital (MO) interaction was between the lowest unoccupied molecular orbital (LUMO) of the $\{C_2B_9H_9\}$ ligand and the highest occupied molecular orbital (HOMO) of the $\{Pt(PH_3)_2\}$ unit. A similar situation, and corresponding conformation, was observed in $\{Pt(PR_3)_2\}$ derivatives of selena- and tellura-boranes $\{XB_{10}H_{10}\}$[5,7] where the $\{SB_{10}H_{10}\}$ ligand was used as the model ligand. In the present case the LUMO of the $\{P_2B_9H_9\}$ ligand is 65% localised on the P_2B_3 face but it has a mirror plane of symmetry bisecting the P–P vector and, if interaction with the PtP_2 unit occurred, it would give a planes-perpendicular conformation [Fig. 2(*b*)]. However, this is not the only possible interaction of consequence because the LUMO+1, which is 0.69 eV higher in energy than the LUMO and 74% localised on the P_2B_3 face, could interact and would give a planes-parallel conformation [Fig. 2(*a*)]. Other interactions with the LUMO+2 and +3 orbitals (1.25 and 1.55 eV higher than the LUMO and 24 and 49% localised on P_2B_3 respectively) could occur to give the conformations shown in Fig. 2(*b*) and 2(*a*) respectively but these are clearly much less likely. It is noteworthy that in the case of the $\{SB_{10}H_{10}\}$ ligand[5,7] the LUMO+1 and +2 orbitals were unsuitable for interaction with PtP_2 either because of their composition (LUMO+1) or energy (LUMO+2 which was 3.64 eV higher than the LUMO).

As far as interactions with occupied orbitals on $\{P_2B_9H_9\}$ are concerned, of the six highest-occupied orbitals only the HOMO and the two orbitals immediately below it have significant electron density in the P_2B_3 face. The HOMO and the HOMO −2 orbital, which is 0.94 eV below, have compositions of 60 and 53% respectively on P_2B_3 face which would lead to planes-parallel conformations. The HOMO−1 orbital which is 0.46 eV below the HOMO has 43% on the P_2B_3 face and would lead to a planes-perpendicular conformation.

From the above analysis it is not possible to offer a simple correlation of the results of the MO calculations and the observed conformation of the PtP_2 unit above the As_2B_3 face in compound **2**. This conclusion is relevant to the molecular structure of **1** and the results of the variable-temperature ^1H NMR study of **2**, discussed below, which indicate that the energetic differences between the various conformers are in any event very small ($< ca.$ 30 kJ mol^{-1}).

(3) *Molecular Structure of* $[3,3\text{-}(PPh_3)_2\text{-closo-}3,1,2\text{-}PtAs_2B_9H_9]$ **1**.—The molecular structure of $[3,3\text{-}(PPh_3)_2\text{-}closo\text{-}3,1,2\text{-}PtAs_2B_9H_9]$ **1** is shown in Fig. 3 and important interatomic distances and angles are given in Table 2. The basic architecture is like that of compound **2**, with the difference that one of the arsenic atoms is exchange-disordered with a BH group over two sites, labelled As(2) and As(4) in Fig. 3. In this respect the structure resembles that of $[3,3\text{-}(PPh_3)_2\text{-}3\text{-}H\text{-}closo\text{-}3,1,2\text{-}RhC_2B_9H_9]$ which shows a similar disorder at the carbon sites.[17] The distances between platinum and the non-disordered arsenic site is 259.1(5) pm which is intermediate between the

Table 2 Selected interatomic distances (pm) and angles (°) for compound **1**

As(1)–Pt(3)	259.1(5)	As/B(2)–Pt(3)	255.7(5)
As/B(4)–Pt(3)	264.0(6)	P(1)–Pt(3)	232.7(5)
P(2)–Pt(3)	232.5(5)	B(8)–Pt(3)	243.4(17)
B(9)–Pt(3)	229.7(18)		
As/B(2)–As(1)	251.5(6)	As/B(4)–As(1)	243.5(5)
B(5)–As(1)	219.8(20)	B(6)–As(1)	217.9(19)
B(6)–As/B(2)	215.2(19)	B(7)–As/B(2)	207.6(19)
B(8)–As/B(2)	217.3(17)	B(5)–As/B(4)	216.2(20)
B(9)–As/B(4)	217.9(19)	B(10)–As/B(4)	198.0(23)
B(6)–B(5)	182.0(26)	B(10)–B(5)	180.9(28)
B(11)–B(5)	174.1(26)	B(7)–B(6)	183.6(25)
B(11)–B(6)	174.3(24)	B(8)–B(7)	191.9(25)
B(11)–B(7)	175.4(25)	B(12)–B(7)	168.3(24)
B(9)–B(8)	190.9(25)	B(12)–B(8)	173.9(24)
B(10)–B(9)	186.3(27)	B(12)–B(9)	187.1(24)
B(11)–B(10)	175.7(27)	B(12)–B(10)	185.1(29)
B(12)–B(11)	170.1(25)		
C(111)–P(1)	183.8(9)	C(211)–P(2)	184.2(9)
C(121)–P(1)	184.1(9)	C(221)–P(2)	185.2(9)
C(131)–P(1)	184.4(9)	C(231)–P(2)	181.6(10)

Angles at Pt(3), As(1), As/B(2), As/B(4), P(1) and P(2)

As(1)–Pt(3)–As/B(2)	58.5(2)	Pt(3)–As(1)–As/B(2)	60.1(2)
B(8)–Pt(3)–As/B(2)	51.4(5)	Pt(3)–As(1)–As/B(4)	63.3(2)
B(8)–Pt(3)–B(9)	47.5(5)	B(5)–As(1)–As/B(4)	55.3(6)
B(9)–Pt(3)–As/B(4)	51.8(5)	B(5)–As(1)–B(6)	49.1(6)
As(1)–Pt(3)–As/B(4)	55.5(2)	B(6)–As(1)–As/B(2)	54.0(6)
As(1)–As/B(2)–Pt(3)	61.4(2)	As(1)–As/B(4)–Pt(3)	61.2(2)
As(1)–As/B(2)–B(6)	55.0(6)	As(1)–As/B(4)–B(5)	56.8(6)
B(6)–As/B(2)–B(7)	51.4(7)	B(5)–As/B(4)–B(10)	51.6(8)
B(7)–As/B(2)–B(8)	53.6(7)	B(9)–As/B(4)–B(10)	53.0(8)
B(8)–As/B(2)–Pt(3)	61.3(5)	B(9)–As/B(4)–Pt(3)	56.0(5)
C(111)–P(1)–Pt(3)	109.6(4)	C(211)–P(2)–Pt(3)	113.2(4)
C(121)–P(1)–Pt(3)	116.6(4)	C(221)–P(2)–Pt(3)	114.3(4)
C(131)–P(1)–Pt(3)	121.6(4)	C(231)–P(2)–Pt(3)	116.2(4)

Angles in the As(1)As/B(2)B(8)B(9)As/B(4) and As/B(2)Pt(3)As/B(4)B(5)B(6) rings below Pt(3) and As(1) respectively

As(1)–As/B(2)–B(8)	101.9(5)	As/B(2)–Pt(3)–As/B(4)	98.0(2)
As/B(2)–B(8)–B(9)	112.4(10)	Pt(3)–As/B(4)–B(5)	101.9(6)
B(8)–B(9)–As/B(4)	122.7(11)	As/B(4)–B(5)–B(6)	117.0(11)
B(9)–As/B(4)–As(1)	98.1(5)	B(5)–B(6)–As/B(2)	121.3(11)
As/B(4)–As(1)–As/B(2)	104.8(2)	B(6)–As/B(2)–Pt(3)	101.7(5)

platinum–arsenic distances in **2**. The other platinum–arsenic distances are 264.0(6) and 255.7(5) pm, showing a similar distortion to that seen in **2**. The platinum–phosphorus distances, 232.7(5) and 232.5(5) pm, are almost identical and possibly slightly longer than those in **2**. The platinum–boron distances to B(8) and B(9) are significantly different being 243.4(17) and 229.7(18) pm respectively. It is noteworthy that the longer Pt–As/B(4) distance is adjacent to the shorter Pt–B(9) interaction and the shorter Pt–As/B(2) is adjacent to the longer Pt–B(8), whereas in **2** above the platinum–boron distances are almost identical.

Interboron distances in compound **1** fall within the range 168.3(25)–191.9(25) pm which is considerably larger than the range in **2** but still within the commonly accepted range of boron–boron bonding distances.[12] The interarsenic distances in **1** were calculated to be 251.5(6) and 243.5(5) pm for As/B(2)–As(1) and As/B(4)–As(1) respectively, comparable with 249.7(3) pm in **2**. The boron–arsenic distances in **1** range from 198.0(23) pm for B(10)–As/B(4) to 219.8(20) pm for B(5)–As(1), the corresponding range in **2** being 210.4(12) to 225.7(11) pm.

Thus the solid-state structure of compound **1** contains a 1:1 mixture of two conformers, Fig. 2(*a*) and 2(*b*). From a study of the variation with temperature of the ^1H-$\{^{31}P\}$ NMR spectra of **2** (see below) it was concluded that the maximum of the energy barrier to free rotation of the PtP_2 unit above the As_2B_3 face of the $\{As_2B_9H_9\}$ ligand is $\leqslant$ *ca.* 40 kJ mol^{-1}. A similar value can be assumed for **1**. It appears that the barrier to rotation is insufficient to discriminate in favour of either of the conformers in Fig. 2 in the crystallisation of **1** whereas for **2** the conformer in Fig. 2(*a*) was preferred. It is possible that in both cases the observed solid-state configuration is dictated by crystal-packing forces rather than electronic control. This observation is of interest in connection with the detailed analysis of the frontier orbitals of $\{Pt(PH_3)_2\}$ and $\{C_2B_9H_{11}\}$ units in related twelve-vertex *closo* platinacarbaboranes.[8] In that study clear conformational preferences could be discerned which correlated with the observed solid-state structures. However, no attempt was made to calculate the energies of the barriers to rotation or the energetic differences between the rotational minima considered, and it should be noted in this context that NMR studies that we have made on [3,3-$(PMe_2Ph)_2$-*closo*-3,1,2-$PtC_2B_9H_{11}$] suggest that this species also has a very low energy ($\leqslant$ *ca.* 40 kJ mol^{-1}) for free rotation.[18] Unfortunately in our hands this last species crystallises with macroscopic disorder that precludes a satisfactory single-crystal diffraction analysis. There is some current interest in examining the cluster distortions exhibited by the solid-state frozen rotamers in other related platinaheteroborane systems which also freely rotate in the fluid phase.[19]

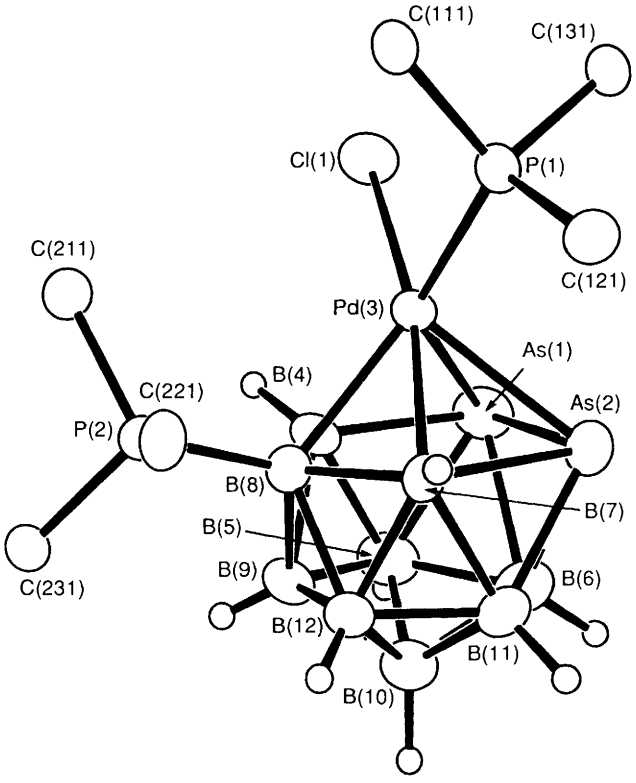

Fig. 4 ORTEP-type diagram of [3-Cl-3,8-$(PPh_3)_2$-*closo*-3,1,2-$PdAs_2B_9H_8$] **5** with P-organyl atoms, other than those attached to phosphorus, omitted for clarity

(4) *Molecular Structure of* [3-Cl-3,8-$(PPh_3)_2$-closo-3,1,2-$PdAs_2B_9H_8$] **5**.—The complex [3-Cl-3,8-$(PPh_3)_2$-*closo*-3,1,2-$PdAs_2B_9H_8$] **5** has the same basic MAs_2B_9 cage structure as those of **1** and **2**. It can also be related to $[B_{12}H_{12}]^{2-}$ using Wade's approach, but contains (*i*) a {B(PPh_3)} group, which is equivalent to $\{BH\}^-$, and (*ii*) the less common {PdCl(PPh_3)} metal unit, which can be regarded as equivalent to a $\{BH\}^+$ unit. The molecular structure is shown in Fig. 4 and important interatomic distances and angles are given in Table 3. Different palladium–arsenic and –boron distances may be expected for each Pd–B–As face since the palladium–chlorine bond is *trans* to Pd–As(2)–B(7) whilst the palladium-phosphorus bond is *trans* to Pd–As(1)–B(4). However, the palladium–boron distances are significantly different only at the 'three times e.s.d. level' being 221.8(8) pm for Pd–B(7) and 229.1(8) pm for Pd–B(4).

The palladium–boron distance involving B(8), at 233.5(8) pm, is notably long compared to the equivalent platinum–boron bond in **2**, 228.1(12) pm. This may be reflection of substantial steric interaction between the PPh_3 ligands in **5** although an electronic cause cannot be excluded. The B(8)–P distance of 194.8(8) pm is also long compared to most of the B–P distances reported for tertiary phosphine ligands pendant to borane clusters.[13]

The palladium–boron distances in compound **5** may be compared with those in some reported [3-L-*closo*-3,1,2-$PdC_2B_9H_{11}$] compounds [L = tmen, **7**;[9] {$(PMe_3)_2$}, **8**;[9] or cod, **9**[10]]. For the distances to B(4), B(7) and B(8), the values are 218.2(6), 218.2(6) and 220.5(5) pm for **7**, 224.9(4), 226.0(5) and 231.5(5) pm for **8**, and 217.8(4), 221.9(3) and 229.4(4) pm for **9** respectively. Hence, in these compounds the differences in the bond distances to B(4) and B(7) are much less marked than those in **5**. It is also clear that phosphine ligands, see **8**, tend to produce longer Pd–B distances. Those in **5** are most like those in **8**.

The palladium–arsenic distances to As(1) and As(2) are 256.3(4) and 253.9(4) pm respectively. Reported two-centre two-electron palladium–arsenic distances are typically in the range from 231.9(1) pm, as in [bis(6-methylquinolin-8-yl)phenylarsine]dichloropalladium,[20] to 245.4(2) pm, as in dichloro[*o*-phenylenebis(dimethylarsine)]palladium(IV) diperchlorate.[21]

The interarsenic distances in compound **5**, 247.7(3) pm, is close to that of 249.7(3) in **2**. As in **2** the arsenic–boron distances are longer when the boron atom is bonded to two heteroatoms. For example As(1)–B(4) [225.0(8) pm] and As(1)–B(6) [222.9(9) pm] are significantly longer than As(1)–B(5) 211.2(9) pm. The situation at As(1) is the same and hence the bonding geometry around both arsenic atoms is remarkably similar.

The interboron distances in compound **5** range from 173.9(12) to 189.6(10) pm. The ranges in compounds **7**–**9** are all smaller being 175.1(8) to 184.8(6), 176.9(7) to 181.6(6) and 173.9(5) to 181.3(5) pm respectively. The larger range in **5** is mainly due to the distortions in that part of the B_9 cage which contains the arsenic atoms.

The palladium–chlorine distance of 240.0(3) pm can be compared with 'typical' values of 236.2(3) and 242.7(5) pm, as

Table 3 Selected interatomic distances (pm) and angles (°) for compound **5**

As(1)–Pd(3)	256.3(4)	As(2)–Pd(3)	253.9(4)
Cl(1)–Pd(3)	240.0(3)	P(1)–Pd(3)	234.4(3)
B(4)–Pd(3)	229.1(8)	B(7)–Pd(3)	221.8(8)
B(8)–Pd(3)	233.5(8)		
As(2)–As(1)	247.7(3)	B(4)–As(1)	225.0(8)
B(5)–As(1)	211.2(9)	B(6)–As(1)	222.9(9)
B(6)–As(2)	222.5(9)	B(7)–As(2)	228.1(8)
B(11)–As(2)	210.1(9)		
B(5)–B(4)	188.9(11)	B(8)–B(4)	177.2(10)
B(9)–B(4)	178.9(10)	B(9)–B(5)	177.1(11)
B(6)–B(5)	184.5(13)	B(11)–B(6)	184.1(12)
B(10)–B(5)	178.7(12)	B(8)–B(7)	180.6(10)
B(10)–B(6)	173.9(12)	B(12)–B(7)	180.6(11)
B(11)–B(7)	189.6(10)	B(9)–B(8)	176.1(10)
B(12)–B(8)	177.1(10)	B(10)–B(9)	176.3(11)
B(12)–B(9)	174.1(12)	B(12)–B(10)	175.9(11)
B(11)–B(10)	178.2(12)	B(12)–B(11)	179.4(11)
B(8)–P(2)	194.8(8)	C(211)–P(2)	180.0(5)
C(221)–P(2)	181.0(5)	C(231)–P(2)	181.2(5)
C(111)–P(1)	182.9(5)	C(121)–P(1)	182.8(5)
C(131)–P(1)	182.9(5)		

Angles at Pd(3), As(1), As(2), B(8), P(1) and P(2)

As(1)–Pd(3)–As(2)	58.1(1)	Pd(3)–P(1)–C(111)	117.9(2)
As(1)–Pd(3)–B(4)	54.9(3)	Pd(3)–P(1)–C(121)	115.3(2)
As(2)–Pd(3)–B(7)	56.8(2)	Pd(3)–P(1)–C(131)	112.1(2)
B(4)–Pd(3)–B(8)	45.0(2)	B(8)–P(2)–C(211)	117.6(3)
B(7)–Pd(3)–B(8)	46.7(2)	B(8)–P(2)–C(221)	108.9(3)
P(1)–Pd(3)–Cl(1)	91.7(2)	B(8)–P(2)–C(231)	113.9(3)
Pd(3)–B(8)–B(4)	66.2(4)	B(7)–B(8)–B(12)	60.6(4)
Pd(3)–B(8)–B(7)	63.2(4)	B(9)–B(8)–B(12)	59.1(5)
B(4)–B(8)–B(9)	60.9(4)		
As(2)–As(1)–Pd(3)	60.5(2)	As(1)–As(2)–Pd(3)	61.4(2)
As(2)–As(1)–Pd(6)	56.1(3)	As(1)–As(2)–B(6)	56.3(3)
Pd(3)–As(1)–B(4)	56.4(3)	Pd(3)–As(2)–B(7)	54.5(2)
B(4)–As(1)–B(5)	51.2(3)	B(7)–As(2)–B(11)	51.1(3)
B(5)–As(1)–B(6)	50.2(4)	B(6)–As(2)–B(11)	50.3(4)

Angles in the As(1)As(2)B(7)B(8)B(4), Pd(3)B(7)B(12)B(9)B(4), Pd(3)B(4)B(5)B(6)As(2) and Pd(3)As(1)B(6)B(11)B(7) rings below Pd(3), B(8), As(1) and As(2) respectively

As(2)–As(1)–B(4)	96.4(3)	Pd(3)–B(7)–B(12)	120.8(5)
As(1)–B(4)–B(8)	119.7(5)	B(7)–B(12)–B(9)	109.4(5)
B(4)–B(8)–B(7)	110.0(5)	B(12)–B(9)–B(4)	109.2(5)
B(8)–B(7)–As(2)	118.8(4)	B(9)–B(4)–Pd(3)	119.4(5)
B(7)–As(2)–As(1)	95.1(3)	B(4)–Pd(3)–B(7)	81.1(3)
Pd(3)–B(4)–B(5)	116.9(5)	Pd(3)–As(1)–B(6)	100.0(3)
B(4)–B(5)–B(6)	112.8(6)	As(1)–B(6)–B(11)	113.6(5)
B(5)–B(6)–As(2)	114.6(5)	B(6)–B(11)–B(7)	113.4(5)
B(6)–As(2)–Pd(3)	100.9(3)	B(11)–B(7)–Pd(3)	117.1(4)
As(2)–Pd(3)–B(4)	93.7(3)	B(7)–Pd(3)–As(1)	94.3(3)

Table 4 Measured NMR parameters for $[3,3\text{-}(PR_3)_2\text{-}closo\text{-}3,1,2\text{-}PtAs_2B_9H_9]$ compounds, R_3 = Ph_3 **1** or Me_2Ph **2** (CD_2Cl_2 solution at 294–297 K)

Assignment/ intensity	$\delta(^{11}B)$		$^1J(^{11}B\text{–}^1H)$	$\delta(^1H)$	
	1[a]	**2**[b]	**2**[a]	**1**	**2**[c]
8 (1)	+12.9[c]	+11.4[d]	130	+4.36	+3.89
10 (1)	+6.9	+5.9	145	+5.81	+6.04[e]
9,12 (2)	+1.6	+1.5	139	+3.31[f]	+3.47[g]
4,7 (2)	+2.8[c]	+0.7[h]	*ca.* 150	+2.00	+2.10
5,11 (2)	−11.7	−12.9	150	+2.57[i]	+2.78[g]
6 (1)	−13.5	−13.7	*ca.* 165	+2.19[j]	+2.63[k]

[a] Additional NMR data: $\delta(^{31}P)$ +22.0, $^1J(^{195}Pt\text{–}^{31}P)$ 3218 ± 8 Hz. Ξ (^{195}Pt) being defined as in ref. 31. [b] Additional NMR data: $\delta(^{31}P)$ −11.2, $^1J(^{195}Pt\text{–}^{31}P)$ 3170 ± 4 Hz; $\delta(^1H)$(PPh) *ca.* +7.45 (3 H) and *ca.* +7.55 (2 H), (PMe_2) +1.85, $^3J(^{195}Pt\text{–}P\text{–}C\text{–}^1H)$ 23.5, $^2J(^{31}P\text{–}^1H)$ 9.5 Hz; at 173 K $\delta(^1H)$ (PMe_2) +1.79 with only marginal broadening. $\delta(^{195}Pt)$ = −857 ppm relative to Ξ 21.4, Ξ being defined as in ref. 31. [c] Satellites due to $^1J(^{195}Pt\text{–}^{11}B)$ apparent. [d] $^1J(^{195}Pt\text{–}^{11}B)$ *ca.* 225 Hz. [e] $^4J(^{195}Pt\text{–}^1H)$ *ca.* 30 Hz. [f] $^3J(^{195}Pt\text{–}^1H)$ 41 ± 7 Hz. [g] $^3J(^{195}Pt\text{–}^1H)$ 37 ± 7 Hz. [h] $^1J(^{195}Pt\text{–}^{11}B)$ *ca.* 85 Hz. [i] $^3J(^{195}Pt\text{–}^1H)$ 43 ± 7 Hz. [j] $^2J(^{195}Pt\text{–}^1H)$ *ca.* 30 Hz. [k] $^2J(^{195}Pt\text{–}^1H)$ 28 ± 7 Hz.

reported for *cis*-$[PdCl_2(PMe_2Ph)_2]$ **10**[22] and *trans*-$[PdCl(H)(PEt_3)_2]$ **11**,[23] respectively. The palladium–phosphorus distance of 234.4(3) pm in **5** compares with values of 228.0(1) and 230.2(1) pm in the *closo*-3,2,1-PdC_2B_9 compound **8**.[9] Palladium–phosphorus distances which have been reported in square-planar complexes include 226.0(2) pm in **10**,[22] 231.0(4) pm in **11**,[23] and 233.3(7) pm in *trans*-$[PdI_2(PMe_2Ph)_2]$.[24]

The inclusion of the $Pd(Cl)PR_3$ unit in compound **5** is unusual although several related nickel– and platinum–halogen units have been reported in polyhedral boron-containing cluster compounds. Examples are [1-Br-1,5-$(PPh_3)_2$-*closo*-1,2,3-$NiC_2Et_2B_4H_3$] **12**,[25] [3-Cl-3,8-$(PPh_3)_2$-*closo*-3,1,2-$NiC_2B_9H_{10}$] **13**,[26] and the *closo*-type species [1-Cl-1,2,2,4-$(PMe_2Ph)_4$-1,2-$Pt_2B_{10}H_9$] **14**.[27] Many examples of compounds with $B(PR_3)$ units have been reported, especially in systems containing metals from the iron, cobalt or nickel groups.[15] Typical compounds include **12**–**14**, as just mentioned, together with [1,2,2-$(PPh_3)_3$-2-H-*closo*-2,10-$IrCB_8H_8$],[28] [1-Cl-1-H-1,-3,5-$(PPh_3)_3$-*closo*-1-RuB_9H_7][29] and [5-(η^6-C_6Me_6)-7-(PR_3)-*nido*-5-RuB_9H_{11}].[30]

(5) *NMR Investigation of the* closo-*Twelve-vertex Compounds* **1**–**6**.—(*a*) *Platinum compounds* **1** *and* **2**. The cluster NMR properties of the $[(PR_3)_2PtAs_2B_9H_9]$ platinum compounds **1** and **2** are strikingly similar (Table 4). The ^{11}B and ^1H resonances were assigned on the basis of relative intensities, relative linewidths, and incidence of coupling to ^{195}Pt, and by comparison with the very similar shielding patterns for the analogous palladium compounds **3** and **4**, for which the assignments were established using [$^1H\text{–}^1H$] correlation spectroscopy (COSY) experiments (see below). The assessment was aided by a more general comparison with the NMR behaviour of reported *closo* twelve-vertex $PtTeB_{10}H_{10}$ and $PtSeB_{10}H_{10}$ compounds.[5,7] Compounds **1** and **2** exhibited 1:1:2:2:2:1 relative intensity patterns in their ^{11}B NMR spectra. No bridging ^1H resonances were observed in the ^1H NMR spectra, consistent with the *closo* geometry of the borane cages, and confirmatory that the crystals selected for the structural work (see above) were representative of the bulk sample. The overall shielding patterns of compounds **1**–**3** are similar to that of [3,3-$(PPh_3)_2$-3-H-*closo*-3,1,2-$RhAs_2B_9H_9$] **15**,[1] the most noteworthy differences (Fig. 5) being in the B(10) and B(4,7) positions, antipodal and adjacent to the metal atom respectively, and at the B(9,12) and B(6) positions, antipodal and adjacent to the two arsenic atoms respectively, suggesting some modification of the metal-to-cage and arsenic-to-cage bonding as the metal varies between rhodium and platinum.

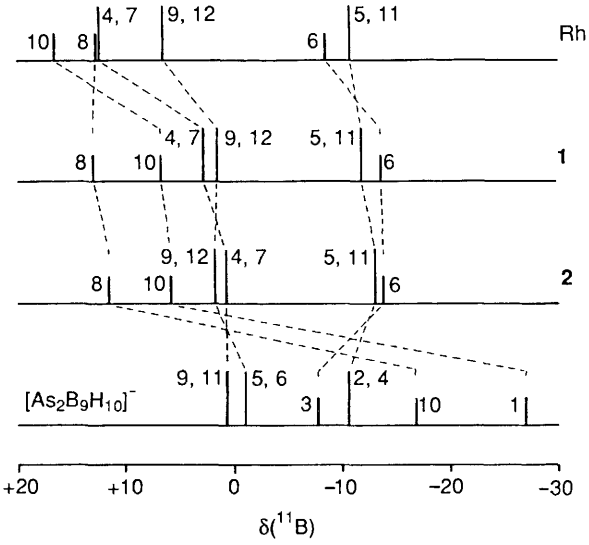

Fig. 5 Stick diagrams of the chemical shifts and relative intensities in the ^{11}B NMR spectra of (centre two traces) $[(PPh_3)_2PtAs_2B_9H_9]$ **1** and $[(PMe_2Ph)_2PtAs_2B_9H_9]$ **2**, together with those of (top) $[(PPh_3)_2HRh\text{-}As_2B_9H_9]$ and (bottom) [*nido*-7,8-$As_2B_9H_{10}]^-$ (data from ref. 1) for comparison. There is a marked similarity among the three metalladirsaboranes, but significant changes compared to the non-metallated ligand precursor (compare ref. 1)

The room-temperature ^1H NMR spectrum of the phosphine ligands in $[3,3\text{-}(PMe_2Ph)_2\text{-}closo\text{-}3,1,2\text{-}PtAs_2B_9H_9]$ **2** exhibited phenyl-group resonance groupings at δ *ca.* +7.5 and only one methyl-group resonance at δ +1.85 (at 294 K). A number of metallaboranes and metallaheteraboranes containing the $\{M(PMe_2Ph)_2\}$ group have been shown by variable-temperature NMR studies to exhibit a rotational fluxionality associated with the metal-to-heteroborane bonding.[1,5,13,18,19] For example, ^1H NMR spectroscopy on the species $[2,2\text{-}(PMe_2Ph)_2\text{-}closo\text{-}2,1\text{-}PtTeB_{10}H_{10}]$[5] reveals two P-methyl resonances at low temperature which coalesce at 290 K (at 9.4 T), giving a value of 58 kJ mol^{-1} for $\Delta G^\ddagger$ for the energy barrier of the fluxional process. However, unexpectedly, the platinadiarsenaborane **2** did not exhibit any significant doubling, or even broadening, of the δ 1.85 resonance in the ^1H NMR spectrum (400 MHz, 9.4 T) that would have implied incipient separation of the P-methyl group resonance, even on cooling to 173 K. Although this observation could result from an accidental coincidence at low temperature of the two chemically distinct prochiral methyl groups, we think this unlikely, and conclude therefore that the $\{Pt(PMe_2Ph)_2\}$ moiety is freely rotating about the 'approximate' Pt(3)–B(10) axis, so that the two methyl groups are on a time-average chemically equivalent.[1,5] This puts an upper limit on $\Delta G^\ddagger$ of *ca.* 30 kJ mol^{-1} (compare ref. 18) and is thereby relevant to the discussion above of the observation that compound **1** exhibits both conformers in Fig. 2 in the crystalline state.

Some of the coupling constants are noteworthy. For instance, $^1J(^{195}Pt\text{–}^{31}P)$ at 3218 ± 8 Hz for **1** and 3170 ± 4 Hz for **2** can be compared to values of 3099 ± 7 and at 2979 ± 6 Hz for [2,2-$(PMe_2Ph)_2$-*closo*-2,1-$PtXB_{10}H_{10}$] (for X = Se and Te, respectively),[5,7] and 3447 ± 7 Hz for [3,3-$(PMe_2Ph)_2$-*closo*-3,1,2-$PtC_2B_9H_{11}$].[18] The coupling $^1J(^{195}Pt\text{–}^{31}P)$ increases with the electronegativity of the transoid groups. For compound **2** the small intracluster coupling $^1J(^{195}Pt\text{–}^{11}B)$ to B(4,7), of only 85 Hz, is interesting, and its small size may imply enhanced platinum bonding to the arsenic atoms at the expense of platinum–boron bonding to the 4,7 positions. Similarly smaller couplings $^1J(^{195}Pt\text{–}^{11}B)$ for platinaheteroboranes in which the platinum atom is bound to a heteroatom have been noted previously.[32,33] However the coupling $^1J(^{195}Pt\text{–}^{11}B)$ of 225 Hz

Table 5 Measured NMR parameters for [3,3-$(PMe_2Ph)_2$-*closo*-3,1,2-$PdAs_2B_9H_9$] **4** and *closo*-[3-Cl-3,8-$(PMe_2Ph)_2$-3,1,2-$PdAs_2B_9H_8$] **6** in CD_2Cl_2 solution at 294 K

Assignment[a]/ intensity	$\delta(^{11}B)$[b]		$^1J(^{11}B-^1H)$[c]/Hz	$\delta(^1H)$[d]		Observed $[^1H-^1H]$ COSY correlations[e]	
	4	**6**	**4**	**4**	**6**	**4**	**6**
4,7 (2)	+10.7	−1.2	143	+2.99	+1.85	(8)w, (9,12)s, (5,11)s	(9,12)m, (5,11)w
8(1)	+10.6	+12.0	—[f]	+3.53	—[g]	(4,7)w, (9,12)s	—
9,12 (2)	+4.5	−0.1	137	+3.28	+2.84	(4,7)s, (8)s, (10)s, (5,11)s	10(w), (5,11)w, (4,7)m
10 (1)	+3.7	−0.2	146	+4.28	+4.05	(9,12)s, (6)w, (5,11)m	(9,12)w, (5,11) s, 6(m)
6 (1)	−7.3	−9.5	160	+2.88	+2.08	(10)m, (5,11)m	(10)m, (5,11)m
5,11 (2)	−12.2	−10.4	150	+2.30	+2.60	(4,7)s, (9,12)s, (10)s, (6)m	s, (9,12)w, (4,7)m, (6)w

[a] Assignment by relative intensities and by $[^1H-^1H]$ COSY cross-peaks. Additional data: **4** $\delta(^{31}P)$ −3.65, $\delta(^1H)$(PMe–Pd)] +1.64, (PPh–Pd)] +7.6 (2 H) and +7.4 (3 H); **6** $\delta(^{31}P)$ = −1.4 and −4.8 [$^1J(^{31}P-^{11}B)$ 135 Hz], $\delta(^1H)$(PMe–Pd) +1.76, (PPh–Pd) +7.6 (2 H) and 7.4 (3 H). [b] ±0.5 ppm to high frequency (low field) of $BF_3(OEt)_2$. [c] ±8 Hz; measured from ^{11}B spectrum with resolution enhancement. [d] ±0.05 ppm to high frequency (low field) of $SiMe_4$. [e] s = Stronger, m = intermediate, w = weaker. [f] Obscured. [g] $\delta(^1H)$ (Me_2PPh) 1.88, $^1J(^{31}P-^1H)$ 12.3 Hz.

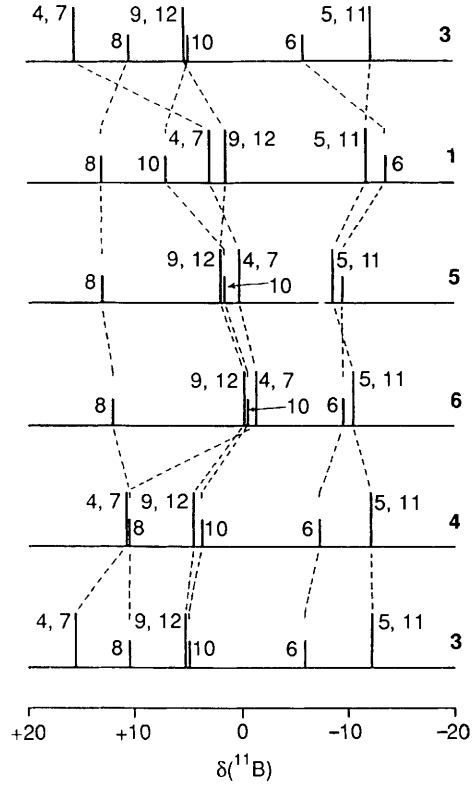

Fig. 6 Stick diagrams of the chemical shifts and relative intensities in the ^{11}B NMR spectra of $[(PPh_3)_2PtAs_2B_9H_9]$ **1**, $[(PPh_3)_2PdAs_2B_9H_9]$ **3**, $[(PMe_2Ph)_2PdAs_2B_9H_9]$ **4**, $[(PPh_3)ClPdAs_2B_9H_8(PPh_3)]$ **5** and $[(PMe_2Ph)ClPdAs_2B_9H_8(PMe_2Ph)]$ **6**. Data for compound **3** are repeated to facilitate comparisons, and dotted lines join equivalent positions in the five molecules

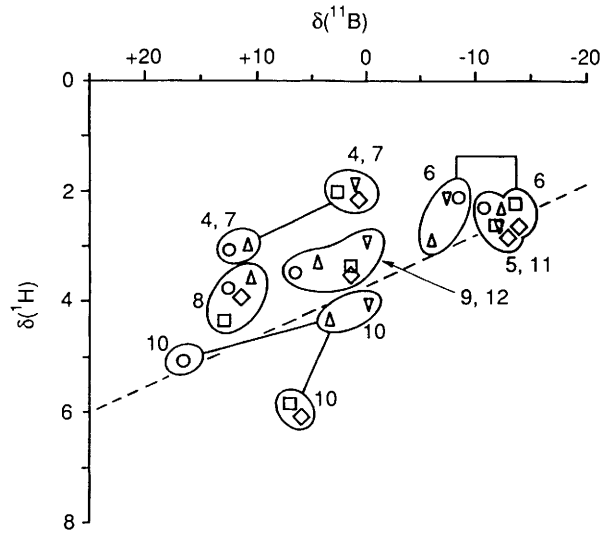

Fig. 7 A plot of $\delta(^1H)$ *versus* $\delta(^{11}B)$ for the BH units of $[(PPh_3)_2PtAs_2B_9H_9]$ **1** (□), $[(PMe_2Ph)_2PtAs_2B_9H_9]$ **2** (◇), $[(PMe_2Ph)_2PdAs_2B_9H_9]$ **4** (△) and $[(PMe_2Ph)ClPdAs_2B_9H_8(PMe_2Ph)]$ **6** (▽), together with those of the rhodium analogue $[(PPh_3)_2HRhAs_2B_9H_9]$ (○) for comparison.[1] The dotted line has slope $\delta(^1H):\delta(^{11}B)$ = 11:1, intercept +3.75 ppm in $\delta(^1H)$ (compare refs. 1, 5–7 and 34–36)

to B(8) in **2** is more within a normal range of values for this type of coupling which has been observed for a variety of non-heteroatom metallaboranes.[33]

(*b*) *Palladium compounds* **3**–**6**. The ^{11}B and ^1H NMR parameters measured for compounds **4** and **6** are summarised in Table 5, and comparative data are plotted in Figs. 6 and 7. Assignments were made in a similar manner to that used for the platinum compounds (see previous sub-section). Although the two chlorinated compounds **5** and **6** are asymmetric and would therefore be expected to have nine separate ^{11}B resonance positions, the ready contrarotational fluxionality of the $\{Cl(PMe_2Ph)\}$ *versus* the $\{As_2B_9H_8(PMe_2Ph)\}$ ligand spheres about the palladium atom (see below) confers a time-average mirror-plane symmetry on the molecules at room temperature in solution so that a 1:1:2:2:2:1 relative intensity pattern is observed.

Fig. 6 is a stick diagram of the ^{11}B NMR spectra of compounds **1** and **3**–**6** with the pattern for $[(PPh_3)_2PdAs_2B_9H_9]$ **3** repeated to facilitate comparisons. It can be seen that the shielding patterns among the platinum and palladium analogues **1**–**4** are very similar, the principal differences between the $\{Pd(PR_3)_2\}$ species **3** and **4** and the corresponding platinum analogues **1** and **2** arising from changes at the 4,7 positions α to the metal atom and a concomitant change at the 6 position β to the metal atom. Other changes among **1**–**4** are relatively minor although it is worth noting that the $^{11}B(10)$ position antipodal to the metal can shift by 5 ppm or so.

The 4,7 positions are also affected considerably upon moving from the $\{Pd(PR_3)_2\}$ species **3** and **4** to the chlorinated $\{PdCl(PR_3)\}$ species **5** and **6**, and it is interesting that the shielding patterns of the latter are thereby rendered very similar to those of the unchlorinated platinum compounds **1** and **2**. There is only a small change in shielding at B(8) on effective hydride–phosphine exchange, a phenomenon that has been previously noted elsewhere, for example in a *nido* ten-vertex $\{RuB_9\}$ system,[37] when neutral PR_3 and anionic hydride ligands are effectively swapped between metal centres and metal-adjacent boron centres.

Aspects of the proton NMR behaviour of compounds **1**–**6** merit comment. Fig. 7 is a plot of $\delta(^{11}B)$ *versus* $\delta(^1H)$ for the BH units of the $\{Pt(PPh_3)_2\}$ and $\{Pt(PMe_2Ph)_2\}$ compounds **1**

and **2** (□ and ◇), the $\{Pd(PMe_2Ph)_2\}$ compound **4** (△), and the $\{PdCl(PMe_2Ph)\}$ compound **6** (▽), together with the previously reported rhodium analogue of **1**, *i.e.* $[3,3\text{-}(PPh_3)_2\text{-}3\text{-}H\text{-}closo\text{-}3,1,2\text{-}RhAs_2B_9H_9]$[1] for comparison (○). The line dotted line drawn, of slope $\delta(^1H):\delta(^{11}B)$ 1:11 and intercept +3.75 ppm in $\delta(^1H)$, has been found to be useful as a benchmark for comparing shielding patterns[1,5–7,34–36] in other twelve-vertex *closo* metallaheteroborane systems. That there is a general overall similarity among all four species is apparent; two groups of $^{11}B^1H(4,7)$ data arise from the differences in ^{11}B behaviour discussed in the previous paragraph, and all (4,7) data are in fact similar in terms of ^1H shielding behaviour in that all lie some −2 ppm in $\delta(^1H)$ from the benchmark line A; the high (4,7) ^1H shielding has been discussed in previous parts of this series.[36] The other spread of data worthy of note in the $^{11}B^1H$ shielding patterns is that for the (10) positions antipodal to the metal atoms. For the $\{RhH(PPh_3)_2\}$ species this arises from a change in ^{11}B shielding,[1] and the ^1H shielding is not anomalous, being close to the dotted line. For the $\{Pt(PMe_2Ph)_2\}$ species the low ^1H shielding is now expected, and is diagnostic[5,7,34–36] for a *closo* twelve-vertex position antipodal to a Period 5 element.

Proton NMR spectroscopy also reveals that the palladium compounds **4** and **6**, and therefore also, by inference, **3** and **5** are fluxional in an analogous way to the platinum compounds **1** and **2** discussed in the previous subsection. All phosphine centres in the two PMe_2Ph palladium compounds examined (**4** and **6**) are prochiral and should therefore exhibit two P-methyl ^1H resonance positions for each phosphine type. This however is contrary to observation at room temperature, indicating fluxionality. For $[(PMe_2Ph)_2PdAs_2B_9H_9]$ **4** no significant broadening of this resonance that could be attributable to an incipient splitting was apparent down to 183 K (400 MHz ^1H spectrum), implying $\Delta G^{\ddagger} < ca.$ 30 kJ mol^{-1}, *i.e.* a very facile fluxionality as inferred also for the platinum compounds **1** and **2** discussed above. The species $[Cl(PMe_2Ph)PdAs_2B_9H_8(PMe_2Ph)]$ **6** did however exhibit elements of broadening at 173 K for the methyl proton resonances of both the Pd- and the B-bound phosphines which, if arising from an incipient splitting, would imply $\Delta G^{\ddagger}$ *ca.* 32 kJ mol^{-1} for the rotational process. Contributions to the restriction producing this higher barrier (for **6** *versus* **2** and **4**) may arise from an eclipsing of the Pd- and B-bound phosphines in the rotational transition state. However, these energies are all relatively low, and it should be borne in mind that any broadening observed at these lower temperatures could also result (in the absence of other evidence) from the freezing out of Pd–P, B–P and P–C bond rotamers.

Experimental

General.—All preparative experiments and recrystallisations were carried out in an inert atmosphere. The platinum complexes $[Pt(PPh_3)_4]$[38] and *cis*-$[PtCl_2(PMe_2Ph)_2]$,[39] the palladium complexes $[PdCl_2(PPh_3)_2]$[40] and $[PdCl_2(PMe_2Ph)_2]$,[41] and the diarsenaboranes $[NMe_4][nido\text{-}7,8\text{-}As_2B_9H_{10}]$ and *closo*-1,2-$As_2B_{10}H_{10}$ were prepared by literature methods.[2,4] In the case of the neutral diarsenaborane significant differences were observed between the reported infrared spectrum and that obtained in the present work: (reported) ν_{max}/cm^{-1} 2450vs, 1440s, 980s, 935s, 760m and 720m; (found) 2500vs, 1470s, 990s, 945s, 760w and 730w. The ^{11}B and ^1H NMR spectra of our sample of $[NMe_4][7,8\text{-}As_2B_9H_{10}]$ agreed with the published data. Infrared spectra were recorded as KBr discs using a Perkin-Elmer 682 Spectrometer. The TLC systems used were as previously described.[7]

Reactions.—$[Pt(PPh_3)_4]$ *with closo*-1,2-$As_2B_{10}H_{10}$. To a solution of 1,2-$As_2B_{10}H_{10}$ (0.14 g, 0.52 mmol) in ethanol (40 cm^3) was added $[Pt(PPh_3)_4]$ (0.59 g, 0.47 mmol). The mixture was stirred at room temperature for 18 h and then refluxed for 24 h. It was concentrated under reduced pressure (rotary film evaporator, 25 °C) and subjected to preparative TLC [CH_2Cl_2–hexane (3:1)]. The major band was extracted into CH_2Cl_2 and recrystallised from this solution as orange plates of $[3,3\text{-}(PPh_3)_2\text{-}closo\text{-}3,1,2\text{-}PtAs_2B_9H_9]$ **1** (0.045 g, 9.3%) (Found: C, 43.10, H, 4.10. $C_{36}H_{39}As_2B_9P_2Pt\cdot0.5CH_2Cl_2$ requires C, 43.05; H, 4.05%). IR: ν_{max}/cm^{-1} 3040w, 2520s(BH), 1580vw, 1567vw, 1474m, 1428s, 1309w, 1180w, 1153vw, 1095s, 1022vw, 994m, 750m, 739s and 691s. NMR data are given in Table 4.

cis-$[PtCl_2(PMe_2Ph)_2]$ *with* $[NMe_4][7,8\text{-}As_2B_9H_{10}]$. Triethylamine (0.4 cm^3, 3.0 mmol) was added to a solution of $[NMe_4][7,8\text{-}As_2B_9H_{10}]$ (0.1 g, 0.30 mmol) in thf (15 cm^3). The solution was stirred at room temperature for *ca.* 10 min, before adding a suspension of $[PtCl_2(PMe_2Ph)_2]$ (0.16 g, 0.30 mmol) in thf (10 cm^3). The mixture was stirred at room temperature for 2 d and then at reflux for 6 h. It was concentrated under reduced pressure (rotary film evaporator, 25 °C) and subjected to preparative TLC [CH_2Cl_2–hexane (4:1)]. The major band was extracted into CH_2Cl_2 and recrystallisation [CH_2Cl_2–cyclohexane (3:1)] yielded red crystals of $[3,3\text{-}(PMe_2Ph)_2\text{-}closo\text{-}3,1,2\text{-}PtAs_2B_9H_9]$ **2** (0.098 g, 44.6%) (Found: C, 26.85; H, 4.20. $C_{16}H_{31}B_9As_2P_2Pt$ requires C, 26.40; H, 4.30%); IR ν_{max}/cm^{-1} 3050w, 2970vw, 2904w, 2530vs(BH), 2505vs(sh)(BH), 2495vs(sh)(BH), 1485w, 1471w, 1430s, 1420m, 1415m, 1400w, 1392w, 1310w, 1297w, 1282m, 1158w, 1101m, 1072w, 1009m, 1000m, 943s, 915vs, 905vs, 860w, 840m, 749s, 739m(sh), 715s, 695m and 681m. NMR data are given in Table 4.

$[PdCl_2(PPh_3)_2]$ *with* $[NMe_4][7,8\text{-}As_2B_9H_{10}]$. *Procedure* 1. To a solution of $[NMe_4][7,8\text{-}As_2B_9H_{10}]$ (0.10 g, 0.30 mmol) in thf (15 cm^3) was added triethylamine (0.4 cm^3, 3.0 mmol). The solution was stirred at room temperature for *ca.* 10 min, then a suspension of $[PdCl_2(PPh_3)_2]$ (0.21 g, 0.30 mmol) in thf (30 cm^3) was added. The mixture was stirred for 48 h at ambient temperature. The green solution was filtered and concentrated under reduced pressure (rotary film evaporator, 25 °C). Preparative TLC [CH_2Cl_2–hexane (3:2)] produced ten bands. Two bands were isolated. The major band was extracted into CH_2Cl_2 and then purified by repeated chromatography [CH_2Cl_2–hexane (4:1)] yielding lavender microcrystals of $[3,3\text{-}(PPh_3)_2\text{-}closo\text{-}3,1,2\text{-}PdAs_2B_9H_9]$ **3** (0.084 g, 31.4%) (Found: C, 49.70; H, 4.30. $C_{36}H_{39}As_2B_9P_2Pd$ requires C, 48.75; H, 4.45%). IR ν_{max}/cm^{-1} 3045w, 2920vw, 2855vw, 2525vs(BH), 1585w, 1570w, 1479m, 1431vs, 1310w, 1186w, 1159w, 1091s, 998s, 751m(sh), 741s and 695vs. NMR data are in Table 5. The minor band was shown to be due to compound **5**, $[3\text{-}Cl\text{-}3,8\text{-}(PPh_3)_2\text{-}closo\text{-}3,1,2\text{-}PdAs_2B_9H_8]$ (see below), isolated in a low yield (0.003 g, 1.1%).

Procedure 2. To a solution of $[NMe_4][7,8\text{-}As_2B_9H_{10}]$ (0.10 g, 0.30 mmol) in thf (20 cm^3) was added triethylamine (0.4 cm^3, 3.0 mmol). The solution was stirred at room temperature for *ca.* 10 min, then a suspension of $[PdCl_2(PPh_3)_2]$ (0.21 g, 0.30 mmol) in thf (20 cm^3) was added. The reaction was stirred at ambient temperature for 16 h and then at refluxed for 20 min. The dark brown solution was filtered and concentrated under reduced pressure (rotary film evaporator, 25 °C). Preparative TLC [CH_2Cl_2–hexane (3:2)] produced twelve bands. The major component was purified by repeated chromatography (100% CH_2Cl_2) and recrystallisation from CH_2Cl_2 solution gave emerald-green blocks of $[3\text{-}Cl\text{-}3,8\text{-}(PPh_3)_2\text{-}closo\text{-}3,1,2\text{-}PdAs_2B_9H_8]$ **5** (0.075 g, 26.8%) (Found: C, 44.9; H, 4.00. $C_{36}H_{38}As_2B_9ClP_2Pd\cdot CH_2Cl_2$ requires C, 44.15; H, 4.00%). IR: ν_{max}/cm^{-1} 3049w, 2920vs, 2841vs, 2560s(BH), 2539s(BH), 2510s(sh)(BH), 1581w, 1570w, 1479s, 1430vs, 1314w, 1262w, 1185w, 1155w, 1090s, 1070w, 1028w, 1015vw, 999w, 980m, 912w, 739s and 695vs. NMR data are in Table 5. A minor component, $[3,3\text{-}(PPh_3)_2\text{-}closo\text{-}3,1,2\text{-}PdAs_2B_9H_9]$ **3**, was isolated in low yield (0.004 g, 1.5%).

$[PdCl_2(PMe_2Ph)_2]$ *with* $[NMe_4][7,8\text{-}As_2B_9H_{10}]$. To a solution of $[NMe_4][7,8\text{-}As_2B_9H_{10}]$ (0.10 g, 0.30 mmol) in thf (15 cm^3) was added triethylamine (0.4 cm^3, 3.0 mmol). The solution was stirred at room temperature for 10 min, then a suspension of $[PdCl_2(PMe_2Ph)_2]$ (0.14 g, 0.3 mmol) in thf (20

Table 6 Crystallographic data for compounds **1**, **2** and **5**[a]

Compound	**1**	**2**	**5**
Formula	$C_{36}H_{39}As_2B_9P_2Pt{\cdot}0.5CH_2Cl_2$	$C_{16}H_{31}As_2B_9P_2Pt$	$C_{36}H_{38}As_2B_9ClP_2Pd{\cdot}CH_2Cl_2$
M	1018.34[b]	727.59	921.66[b]
a/pm	1230.0(2)	1308.6(3)	1037.8(2)
b/pm	1736.5(4)	1058.0(2)	1321.9(3)
c/pm	1881.0(3)	1934.7(3)	1712.9(3)
α/°	—	—	103.67(1)
β/°	91.44(2)	104.45(2)	93.19(1)
γ/°	—	—	110.86(1)
U/nm^3	4.0160(13)	2.5938(9)	2.1081(6)
D_c/g cm^{-3}	1.68	1.86	1.59
Crystal system	Monoclinic	Monoclinic	Triclinic
Space group	$P2_1/n$	$P2_1/n$	$P\bar{1}$
Z	4	4	2
$F(000)$	1980	1383	1000
μ/cm^{-1}	50.84	77.81	21.1
No. of data collected	5625	4969	5665
No. observed [$I > 2.0\sigma(I)$]	4160	3778	4688
θ_{min},θ_{max}/°	2.0, 22.5	2.0, 25.0	2,0, 25.0
R	0.0574	0.0384	0.0392
R'	0.0532	0.0376	0.0408
Weighting factor g	0.0001	0.0002	0.0003
No. of variables	176	296	445

[a] For all three compounds: scan width 2.0° + α − doublet splitting; scan speeds 2.0–29.3° min^{-1}. [b] Includes solvate molecule(s).

Table 7 Non-hydrogen atom coordinates ($\times 10^4$) for [3,3-$(PPh_3)_2$-*closo*-3,1,2-$PtAsB_9H_9$] **1**

Atom	x	y	z	Atom	x	y	z
Pt(3)	501.1(4)	2155.2(3)	1241.1(2)	C(212)	−3101(7)	1255(4)	1268(5)
As(1)	1292(1)	1283(1)	265(1)	C(213)	−3630(7)	591(4)	1493(5)
As/B(2)	1156(2)	2711(2)	69(1)	C(214)	−3063(7)	−102(4)	1546(5)
As/B(4)	2078(2)	1147(2)	1458(2)	C(215)	−1968(7)	−132(4)	1375(5)
P(1)	−25(3)	2160(2)	2420(2)	C(216)	−1439(7)	532(4)	1151(5)
P(2)	−1241(3)	2046(2)	747(2)	C(221)	−1284(7)	1865(5)	−223(3)
C(111)	624(7)	1354(4)	2897(4)	C(222)	−1308(7)	2497(5)	−679(3)
C(112)	1376(7)	1462(4)	3454(4)	C(223)	−1318(7)	2385(5)	−1413(3)
C(113)	1838(7)	827(4)	3800(4)	C(224)	−1304(7)	1641(5)	−1690(3)
C(114)	1547(7)	85(4)	3588(4)	C(225)	−1280(7)	1009(5)	−1233(3)
C(115)	795(7)	−24(4)	3031(4)	C(226)	−1270(7)	1121(5)	−500(3)
C(116)	334(7)	611(4)	2685(4)	C(231)	−2078(7)	2905(5)	773(5)
C(121)	306(7)	3029(4)	2940(4)	C(232)	−1633(7)	3572(5)	1071(5)
C(122)	755(7)	3670(4)	2610(4)	C(233)	−2259(7)	4238(5)	1112(5)
C(123)	1030(7)	4319(4)	3010(4)	C(234)	−3332(7)	4237(5)	856(5)
C(124)	857(7)	4329(4)	3739(4)	C(235)	−3778(7)	3570(5)	558(5)
C(125)	409(7)	3689(4)	4069(4)	C(236)	−3151(7)	2904(5)	516(5)
C(126)	133(7)	3039(4)	3669(4)	B(5)	3042(14)	1305(11)	525(10)
C(131)	−1465(6)	2084(6)	2658(5)	B(6)	2579(13)	2027(10)	−112(9)
C(132)	−2100(6)	2740(6)	2553(5)	B(7)	2774(14)	2989(10)	272(9)
C(133)	−3190(6)	2737(6)	2740(5)	B(8)	1843(12)	3160(9)	1059(8)
C(134)	−3644(6)	2076(6)	3031(5)	B(9)	2209(13)	2364(9)	1721(8)
C(135)	−3008(6)	1420(6)	3136(5)	B(10)	3359(17)	1819(12)	1339(11)
C(136)	−1919(6)	1423(6)	2949(5)	B(11)	3626(13)	2216(10)	503(8)
C(211)	−2006(7)	1225(4)	1098(5)	B(12)	3185(13)	2850(10)	1121(8)

cm^3) was added. The reaction mixture was stirred at ambient temperature for 36 h. The brown solution was filtered, concentrated under reduced pressure (rotary film evaporator, 25 °C) and subjected to preparative TLC (CH_2Cl_2–hexane, 4:1) which produced ten bands. The two major bands were extracted into CH_2Cl_2 yielding a wine-coloured solid (R_f = 0.71) and a green solid (R_f = 0.49).

(*a*) The wine-coloured solid was purified by repeated chromatography (100% CH_2Cl_2) and recrystallisation from CH_2Cl_2 afforded [3,3-$(PMe_2Ph)_2$-*closo*-3,1,2-$PdAs_2B_9H_9$] **4** (0.078 g, 40.5%) (Found: C, 30.40; H, 4.60; B, 15.35. $C_{16}H_{31}As_2B_9P_2Pd$ requires C, 30.05; H, 4.90; B, 15.20%). IR: ν_{max}/cm^{-1} 3070vw, 3042w, 2972w, 2910w, 2558s(sh)(BH), 2520vs(BH), 2488s(sh)(BH), 1570w, 1481w, 1431s, 1415m, 1405w(sh), 1310w, 1295vw, 1281w, 1155vw, 1095m, 1070w, 990m, 945s, 909s, 901s, 748s, 729m, 710w and 693s. NMR data are given in Table 5.

(*b*) The green solid was purified by repeated chromatography [CH_2Cl_2–hexane (4:1)] and then recrystallisation from CH_2Cl_2 solution gave [3-Cl-3,8-$(PMe_2Ph)_2$-*closo*-3,1,2-$PdAs_2B_9H_8$] **6** (0.04 g, 19.7%) (Found: C, 28.35; H, 4.25; Cl, 4.90. $C_{16}H_{31}As_2B_9ClP_2Pd$ requires C, 28.55; H, 4.50; Cl, 5.25%). IR: ν_{max}/cm^{-1} 3070vw, 3055w, 2985w, 2903w, 2550s(BH), 2540s(BH), 2517vs(BH), 1570vw, 1481w, 1431s, 1418m, 1408m, 1314w, 1300vw, 1285m, 1278w, 1155w, 1110m, 1070vw, 1018w, 1000w, 998m, 960s, 945s, 918s, 909vs, 863m, 758m, 741m, 729m, 718m, 691s and 681w. NMR data are given in Table 5.

Single-crystal X-Ray Diffraction Analysis.—All crystallographic measurements were made on a Nicolet P3/F

diffractometer operating in the ω–2θ scan mode using graphite-monochromated Mo-Kα radiation (λ = 71.069 pm) following a standard procedure.[42] All three data sets were corrected for absorption empirically once their structures had been determined.[43]

All structures were solved by standard heavy-atom methods and were refined by full-matrix least-squares using the SHELX program system.[44] In the case of compound **1** one of the two cage arsenic atoms was found to be disordered over the 2 and 4 positions. Both positions were consequently refined as 50:50 mixtures of As and B atoms. A solvent molecule, which was disordered about the centre of symmetry at (0,$\frac{1}{2}$,0), was also located. The phenyl rings were treated as rigid bodies with idealised hexagonal symmetry (C–C 139.5 pm). Only the Pd, As, As/B and P atoms were assigned anisotropic thermal parameters; all other atoms were refined isotropically. No hydrogen atoms were located. In the cases of **2** and **5** all non-hydrogen atoms were refined with anisotropic thermal parameters (except for two solvent molecules in **5** which were found to be disordered about the centres of symmetry at 0,$\frac{1}{2}$,0 and 0,0,$\frac{1}{2}$ respectively). As for **1**, phenyl rings were treated as rigid bodies with idealised hexagonal symmetry. All phenyl and methyl hydrogen atoms were included in calculated positions (C–H 96 pm) and were assigned an overall isotropic thermal parameter. Cluster hydrogen atoms were located on Fourier difference syntheses and were refined with individual isotropic thermal parameters. The weighting scheme $w = [\sigma^2(F_o) + g(F_o)^2]^{-1}$ was used for all three compounds in which the parameter g was included in refinement in order to obtain a flat analysis of variance for increasing sin θ and $(F/F_{max})^{\frac{1}{2}}$. Crystal data, data collection and structure refinement parameters are given in Table 6 while atomic coordinates for compounds **1**, **2** and **5** are given in Tables 7, 8 and 9 respectively.

Additional material available from the Cambridge Crystallographic Data Centre comprises H-atom coordinates, thermal parameters and remaining bond lengths and angles.

NMR Spectroscopy.—NMR spectroscopy was performed at 9.4 T on commercially available Bruker AM400 instrumentation, with the general techniques, and the ^{1}H-{^{11}B} and COSY techniques, being essentially as described and illustrated in previous papers in this series.[1,5–7] Chemical shifts δ are given in ppm to high frequency (low field) of Ξ 100 ($SiMe_4$) for ^{1}H, Ξ 40.480 730 (nominally 85% H_3PO_4) for ^{31}P, and Ξ 32.083 971 MHz [nominally $BF_3(OEt_2)$ in $CDCl_3$] for ^{11}B, Ξ being defined as in ref. 31. Solvent deuteron or residual proton resonances were used as internal secondary standards. Coupling constants $^1J(^{11}B–^1H)$ are measured from resolution-enhanced ^{11}B spectra of digital resolution 8 Hz.

Table 8 Non-hydrogen atom coordinates ($\times 10^4$) for [3,3-$(PMe_2Ph)_2$-*closo*-3,1,2-$PtAs_2B_9H_9$] **2**

Atom	*x*	*y*	*z*
Pt(3)	4562.5(2)	5720.4(3)	2269.3(2)
As(1)	2986.0(7)	4247.9(8)	1593.2(5)
As(2)	2738.2(6)	5800.7(9)	2510.0(4)
P(1)	5315(2)	6117(2)	3456(1)
P(2)	5994(2)	4735(2)	2025(1)
B(4)	3838(8)	5605(9)	1071(5)
B(5)	2383(9)	5465(12)	718(5)
B(6)	1692(8)	5678(10)	1392(5)
B(7)	3517(7)	7482(9)	2142(5)
B(8)	4103(8)	7225(9)	1403(6)
B(9)	3075(8)	6877(10)	649(5)
B(10)	1838(8)	6940(11)	853(5)
B(11)	2085(7)	7242(10)	1785(5)
B(12)	2855(8)	7969(11)	1280(5)
C(11)	4426(7)	6548(11)	4005(5)
C(12)	6171(8)	7487(8)	3551(6)
C(131)	6077(4)	4887(5)	4005(3)
C(132)	5670(4)	3663(5)	3932(3)
C(133)	6248(4)	2674(5)	4319(3)
C(134)	7234(4)	2910(5)	4780(3)
C(135)	7641(4)	4135(5)	4853(3)
C(136)	7063(4)	5124(5)	4465(3)
C(21)	7187(6)	4454(11)	2722(5)
C(22)	6542(8)	5586(9)	1390(6)
C(231)	5682(4)	3152(4)	1673(3)
C(232)	5722(4)	2835(4)	980(3)
C(233)	5472(4)	1611(4)	726(3)
C(234)	5182(4)	704(4)	1165(3)
C(235)	5143(4)	1021(4)	1858(3)
C(236)	5392(4)	2245(4)	2112(3)

Table 9 Non-hydrogen atom coordinates ($\times 10^4$) for [3-Cl-3,8-$(PPh_3)_2$-*closo*-3,1,2-$PdAs_2B_9H_8$] **5**

Atom	*x*	*y*	*z*	Atom	*x*	*y*	*z*
Pd(3)	2784.1(4)	2333.5(3)	2616.5(2)	C(126)	2944(3)	3504(3)	454(2)
As(1)	250.3(6)	1197.3(5)	2721.0(4)	C(131)	2971(3)	4823(3)	2200(2)
As(2)	918.0(6)	1315.6(5)	1370.0(4)	C(132)	3595(3)	5862(3)	2040(2)
Cl(1)	2783(2)	3569(1)	3893(1)	C(133)	2913(3)	6611(3)	2131(2)
P(1)	3888(1)	3858(1)	2095(1)	C(134)	1606(3)	6321(3)	2383(2)
P(2)	5283(1)	1002(1)	2900(1)	C(135)	981(3)	5282(3)	2543(2)
B(4)	2080(7)	850(5)	3185(4)	C(136)	1663(3)	4533(3)	2452(2)
B(5)	395(7)	−366(6)	2656(5)	C(211)	6201(3)	2126(3)	3802(2)
B(6)	−226(7)	−293(6)	1662(5)	C(212)	5552(3)	2774(3)	4256(2)
B(7)	2922(6)	1010(5)	1590(4)	C(213)	6307(3)	3642(3)	4948(2)
B(8)	3359(6)	763(5)	2543(4)	C(214)	7710(3)	3861(3)	5184(2)
B(9)	2039(7)	−491(5)	2615(4)	C(215)	8358(3)	3213(3)	4730(2)
B(10)	781(7)	−1089(6)	1741(5)	C(216)	7604(3)	2345(3)	4039(2)
B(11)	1233(7)	−209(5)	1077(4)	C(221)	6290(3)	1295(3)	2094(2)
B(12)	2551(6)	−395(5)	1674(4)	C(222)	7226(3)	2387(3)	2167(2)
C(111)	5682(3)	4793(2)	2557(2)	C(223)	7946(3)	2629(3)	1528(2)
C(112)	6623(3)	5377(2)	2115(2)	C(224)	7729(3)	1779(3)	815(2)
C(113)	7941(3)	6155(2)	2505(2)	C(225)	6794(3)	687(3)	741(2)
C(114)	8316(3)	6349(2)	3338(2)	C(226)	6074(3)	445(3)	1381(2)
C(115)	7375(3)	5765(2)	3780(2)	C(231)	5481(4)	−179(2)	3179(2)
C(116)	6058(3)	4987(2)	3389(2)	C(232)	4775(4)	−508(2)	3802(2)
C(121)	3970(3)	3492(3)	1009(2)	C(233)	4935(4)	−1367(2)	4089(2)
C(122)	5004(3)	3117(3)	732(2)	C(234)	5801(4)	−1896(2)	3752(2)
C(123)	5012(3)	2755(3)	−101(2)	C(235)	6507(4)	−1567(2)	3129(2)
C(124)	3986(3)	2767(3)	−657(2)	C(236)	6347(4)	−709(2)	2842(2)
C(125)	2952(3)	3141(3)	−379(2)				

MNDO calculations were performed with the program devised by Dewar and Thiel.[45]

Acknowledgements

We thank the SERC for support and the Department of Education of the Republic of Ireland for a Senior Studentship (for M. M.). We thank Professor N. N. Greenwood for his interest in some of the initial stages of this work. A generous loan of palladium and platinum salts from Johnson Matthey plc is gratefully acknowledged.

References

1 Part 8, X. L. R. Fontaine, J. D. Kennedy, M. McGrath and T. R. Spalding, *Magn. Reson. Chem.*, 1991, **29**, 711.
2 J. L. Little, S. S. Pao and K. K. Sugathan, *Inorg. Chem.*, 1974, **13**, 1752.
3 J. L. Little and S. S. Pao, *Inorg. Chem.*, 1978, **17**, 584.
4 T. P. Hanusa, N. R. de Parisi, J. G. Kester, A. Arafat and L. J. Todd, *Inorg. Chem.*, 1987, **26**, 4100.
5 G. Ferguson, J. D. Kennedy, X. L. R. Fontaine, Faridoon and T. R. Spalding, *J. Chem. Soc., Dalton Trans.*, 1988, 2555.
6 Faridoon, O. Ni Dhubhghaill, T. R. Spalding, G. Ferguson, B. Kaitner, X. L. R. Fontaine, J. D. Kennedy and D. Reed, *J. Chem. Soc., Dalton Trans.*, 1988, 2739.
7 Faridoon, O. Ni Dhubhghaill, T. R. Spalding, G. Ferguson, B. Kaitner, X. L. R. Fontaine and J. D. Kennedy, *J. Chem. Soc., Dalton Trans.*, 1989, 1657.
8 D. M. P. Mingos, M. I. Forsyth and A. J. Welch, *J. Chem. Soc., Dalton Trans.*, 1978, 1363.
9 H. M. Colquhoun, T. J. Greenhough and M. G. H. Wallbridge, *J. Chem. Soc., Dalton Trans.*, 1985, 761.
10 D. E. Smith and A. J. Welch, *Acta Crystallogr., Sect. C*, 1986, **42**, 117.
11 J. A. Rahn, D. J. O'Donnell, A. R. Palmer and J. H. Nelson, *Inorg. Chem.*, 1989, **28**, 2631 and refs. therein.
12 K. Wade, *Adv. Inorg. Chem. Radiochem.*, 1976, **18**, 1.
13 J. D. Kennedy, *Prog. Inorg. Chem.*, 1986, **34**, 211 and refs. therein.
14 M. K. Cooper, P. J. Guerney and M. McPartlin, *J. Chem. Soc., Dalton Trans.*, 1980, 349.
15 D. R. Russell and P. A. Tucker, *J. Chem. Soc., Dalton Trans.*, 1975, 1752.
16 A. L. Rheingold and P. J. Sullivan, *Organometallics*, 1983, **2**, 327 and refs. therein.
17 G. E. Hardy, K. P. Callaghan, C. E. Strouse and M. F. Hawthorne, *Acta Crystallogr., Sect. B*, 1976, **32**, 264.
18 J. D. Kennedy, X. L. R. Fontaine and J. L. Spencer, unpublished work, University of Leeds, 1986.
19 J. D. Kennedy, B. Stibr, M. Thornton-Pett and T. Jelinek, *Inorg. Chem.*, 1991, in the press.
20 G. L. Roberts, B. W. Skelton, A. H. White and S. B. Wild, *Aust. J. Chem.*, 1982, **25**, 2193.
21 L. R. Gray, D. J. Gulliver, W. Levason and M. Webster, *J. Chem. Soc., Dalton Trans.*, 1983, 133 and refs. therein.
22 L. L. Martin and R. A. Jackobsen, *Inorg. Chem.*, 1971, **10**, 1795.
23 M. L. Schneider and H. M. M. Shearer, *J. Chem. Soc., Dalton Trans.*, 1973, 354.
24 N. A. Bailey and R. Mason, *J. Chem. Soc.*, 1968, 2594.
25 H. A. Boyter, R. G. Swisher, E. Sinn and R. N. Grimes, *Inorg. Chem.*, 1985, **24**, 3810.
26 R. E. King, S. B. Miller, C. B. Knobler and M. F. Hawthorne, *Inorg. Chem.*, 1983, **22**, 3548.
27 Y. M. Cheek, J. D. Kennedy and M. Thornton-Pett, *Inorg. Chim. Acta*, 1985, **99**, L43.
28 N. W. Alcock, J. G. Taylor and M. G. H. Wallbridge, *J. Chem. Soc., Chem. Commun.*, 1983, 1168.
29 J. E. Crook, M. Elrington, N. N. Greenwood, J. D. Kennedy, M. Thornton-Pett and J. D. Woollins, *J. Chem. Soc., Dalton Trans.*, 1985, 2407.
30 M. Bown, X. L. R. Fontaine, N. N. Greenwood and J. D. Kennedy, *J. Organomet. Chem.*, 1987, **325**, 233.
31 W. McFarlane, *Proc. R. Soc. London, Sect. A*, 1968, **306**, 185.
32 B. Wrackmeyer, personal communication (to J. D. K.), 1986.
33 J. D. Kennedy, in *Multinuclear NMR*, ed. J. Mason, Plenum, London and New York, 1987, ch. 8 and refs. therein.
34 S. R. Bunkhall, X. L. R. Fontaine, N. N. Greenwood, J. D. Kennedy and M. Thornton-Pett, *J. Chem. Soc., Dalton Trans.*, 1990, 73.
35 K. Nestor, T. Jelinek, X. L. R. Fontaine, N. N. Greenwood, J. D. Kennedy, M. Thornton-Pett, S. Hermanek and B. Stibr, *J. Chem. Soc., Dalton Trans.*, 1990, 681.
36 Faridoon, M. McGrath, T. R. Spalding, X. L. R. Fontaine, J. D. Kennedy and M. Thornton-Pett., *J. Chem. Soc., Dalton Trans.*, 1990, 1819.
37 N. N. Greenwood, J. D. Kennedy, M. Thornton-Pett and J. D. Woollins, *J. Chem. Soc., Dalton Trans.*, 1985, 2397.
38 R. Ugo, E. Cariati and G. La Monica, *Inorg. Synth.*, 1968, **11**, 105.
39 G. W. Parshall, *Inorg. Synth.*, 1970, **12**, 26.
40 J. R. Blackburn, R. Nordberg, F. Stevie, R. G. Albridge and M. M. Jones, *Inorg. Chem.*, 1970, **9**, 2374.
41 J. M. Jenkins and B. L. Shaw, *J. Chem. Soc. A*, 1966, 770.
42 A. Modinos and P. Woodward, *J. Chem. Soc., Dalton Trans.*, 1974, 2065.
43 N. Walker and D. Stuart, *Acta Crystallogr., Sect. A*, 1983, **39**, 158.
44 G. M. Sheldrick, SHELX 76, Program System for X-Ray Structure Determination, University of Cambridge, 1976.
45 M. J. S. Dewar and W. Thiel, *J. Am. Chem. Soc.*, 1977, **99**, 2531; W. Thiel, Quantum Chemistry Program Exchange, Indiana State University, Bloomington, 1978, vol. 11, p. 353.

Received 23rd *January* 1991; *Paper* 1/00353D